ELSEVIER

Available online at www.sciencedirect.com
SCIENCE DIRECT

Journal of Crystal Growth 249 (2003) 72–77

JOURNAL OF CRYSTAL GROWTH

www.elsevier.com/locate/jcrysgro

Structural and optical properties of InAlGaN films grown directly on low-temperature buffer layer with (0 0 0 1) sapphire substrate

Dabing Li[a,*], Xun Dong[a], Jinsong Huang[b], Xianglin Liu[a], Zhongying Xu[b], Xiaohui Wang[a], Ze Zhang[c], Zhanguo Wang[a]

[a] *Key laboratory of Semiconductor Materials, Institute of Semiconductors, Chinese Academy of Sciences, P.O. Box 912, Beijing 100083, People's Republic of China*

[b] *State Key Laboratory for Superlattices and Microstructures, Institute of Semiconductors, Chinese Academy of Sciences, P.O. Box 912, Beijing 100083, People's Republic of China*

[c] *Beijing Laboratory of Electron Microscopy, Institute of Physics, Chinese Academy of Sciences, Beijing 100080, People's Republic of China*

Received 16 October 2002; accepted 23 October 2002
Communicated by M. Schieber

Abstract

Quaternary InAlGaN film has been grown directly on top of low-temperature-deposited GaN buffer layer by low-pressure metalorganic vapor phase epitaxy. High-resolution X-ray diffraction and photoluminescence (PL) results show that the film has good crystal quality and optical property. Temperature-dependent PL and time-resolved PL (TRPL) have been employed to study the carriers recombination dynamics in the film. The TRPL signals can be well fitted as a *stretched exponential* function $\exp[-(t/\tau)^{\beta}]$ from 14 to 250 K, indicating that the emission is attributed to the radiative recombination of excitons localized in disorder quantum nanostructures such as quantum disks originating from indium (In) clusters or In composition fluctuation. The cross-sectional high-resolution electron microscopy measurement further proves that there exist the disorder quantum nanostructures in the quaternary. By investigating the dependence of the exponential parameter β on the temperature, it is shown that the multiple trapping–detrapping mechanism dominates the diffusion among the localized states. The localized states are considered to have two-dimensional density of states (DOS) at 250 K, since radiative recombination lifetime τ_r increases linearly with increasing temperature.
© 2002 Elsevier Science B.V. All rights reserved.

PACS: 78.47.+p; 81.05.Ea; 81.15.Gh

Keywords: A1. Nanostructures; A1. Stretched exponential; A1. Time-resolved photoluminescence; A3. Metalorganic vapor phase epitaxy; B1. Nitrides; B2. InAlGaN

1. Introduction

Recently, III-group nitrides have attracted much attention because of their many applications

*Corresponding author. Tel./fax: +86-10-8230-4968.
E-mail address: dbli@red.semi.ac.cn (D. Li).

0022-0248/03/$ - see front matter © 2002 Elsevier Science B.V. All rights reserved.
PII: S 0 0 2 2 - 0 2 4 8 (0 2) 0 2 1 0 1 - 2

for optoelectronic devices operating in blue–green to ultraviolet range [1]. Device-quality binary GaN is currently grown by a two-step method [2,3], also great progress has been made in the fabrication of high-quality ternary InGaN and AlGaN together with their related multiple quantum wells (MQWs), light-emitting diodes (LEDs), laser diodes (LDs) and UV photodetectors [1,4]. It has been indicated that the most nitride devices must take advantages of the InGaN/(Al)GaN or GaN/AlGaN MQWs and heterostructures. However, the large lattice mismatch between these two ternary/binary alloys has limited the In or Al content in the MQWs or heterostructure and the thickness of well [5,6]. Moreover, the mismatch arises piezoelectric field that influenced the emission intensity or quantum efficiency (QE) [7]. To avoid such limitation, researchers have developed lattice and bandgap engineering by using quaternary alloys $In_xAl_yGa_{1-x-y}N$ to replace the AlGaN or GaN as barrier [8]. Theoretically, the bandgap and the lattice constants of $In_xAl_yGa_{1-x-y}N$ can each be independently adjusted by varying In and Al compositions, so one can obtain lattice-matched QWs and heterostructures under the required bandgap energy. Besides, the thermal coefficient of $In_xAl_yGa_{1-x-y}N$ is better matched to GaN than to AlGaN, which could be an important advantage in epitaxial growth [9,10]. Several groups have grown $In_xAl_yGa_{1-x-y}N$ alloys with high structural and optical properties on GaN template by MOCVD or MBE and investigated their luminescence mechanism [8,9,11–13]. However, to our knowledge, besides the report of Oder et al. [10] on the photoresponse versus the excitation light wavelength of the InAlGaN grown directly on the thin buffer layer, there are no further studies of InAlGaN grown directly on buffer layer in detail.

In this work we have performed high-resolution X-ray diffraction (HRXRD), time-resolved photoluminescence (TRPL) and high-resolution transmission electron microscopy (HRTEM) studies for InAlGaN film grown directly on top of the thin low-temperature (LT) GaN buffer layer with (0 0 0 1) sapphire substrate. HRXRD results indicate that the film is single crystal; TRPL data show that there exist dispersed In clusters (quantum dots or quantum disks (Q-disks)) in the film; and HRTEM also observes the In clusters resulted from In composition fluctuation, which further supports the TRPL results.

2. Experimental procedures

The growth was conducted at 76 Torr on a (0 0 0 1)-face sapphire substrate. The substrates were first ultrasonically cleaned in organic solvents, rinsed with de-ionized water, dried naturally under an infrared light lamp, details are in Ref. [14], and loaded into a horizontal low-pressure metalorganic phase vapor epitaxy (LPMOVPE) reactor. They were then thermally cleaned in hydrogen (H_2) ambient for 20 min at 1050°C, and followed by a 3 min nitridation in an ammonia (NH_3) flow at 1050°C. After a ~20-nm-thick LT-GaN buffer layer was deposited at 550°C, the growth temperature was increased to 830°C, the optimal growth temperature, for the quaternary InAlGaN epitaxy (Sample No. Y0230). Ethyldmethylidium (EDMIn), trimethylaluminium (TMAl), trimethylgallium (TMGa) and NH_3 were used as In, Al Ga and N precursors, respectively. Nitrogen (N_2) was employed as carrier gas. An InAlGaN film (Sample No. Y0227) was grown on 1.0 μm GaN-template/sapphire substrate for the purpose of comparison.

Transmission electron microscope (TEM) was used to measure the thickness of the epilayers. HRTEM in a CM200-FEG TEM with a point resolution of 0.23 nm and a line resolution of 0.1 nm was employed to evaluate the microstructure of the quaternary film. HRXRD, using synchrotron radiation as a light source, was carried out to investigate the crystal properties. For TRPL measurements, the PL was excited by frequency-doubled ($\lambda = 360$ nm) laser pulses from a Ti:Sapphire mode-locked femtosecond laser, and the time-correlated signals were analyzed by a two-dimensional (2D) synchronous streak camera with an overall resolution of better than 15 ps. PL measurement was performed in cw configuration using a combination of a cooled GaAs photomultiplier tube with a Data-Link electronic system.

3. Results and discussion

Thickness of the quaternary films obtained from TEM is 0.6–0.7 μm. Fig. 1(a) shows the (0 0 0 2) $\theta-2\theta$ HRXRD scans for InAlGaN films grown on GaN-buffer/sapphire substrate (Sample No. Y0230) and GaN-template/sapphire substrate (Sample No. Y0227), respectively. It is observed that there exists no obvious difference between the InAlGaN-related peaks. Comparing LT PL spectra taken at 14 K of the two samples (Fig. 1(b)), we can find that at the same emission energy (3.1 eV), the PL intensity of Sample No. Y0230 is stronger than that of Sample No. Y0227. From the above results, it is concluded that the same quality InAlGaN epifilm, compared with the InAlGaN grown on GaN template/sapphire, can also be deposited directly on LT buffer layer with sapphire substrate.

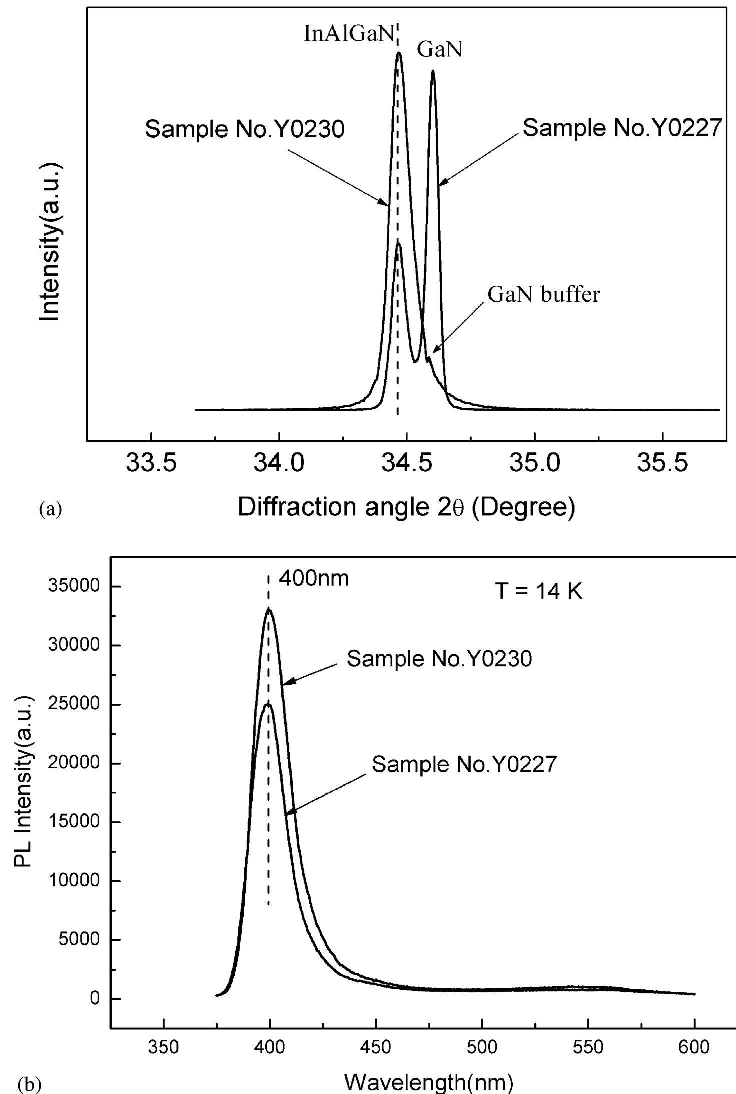

Fig. 1. θ-2θ X-ray diffraction spectra (a) and LT PL spectra (b) of InAlGaN grown on GaN buffer layer with sapphire substrate and GaN-template/sapphire, respectively.

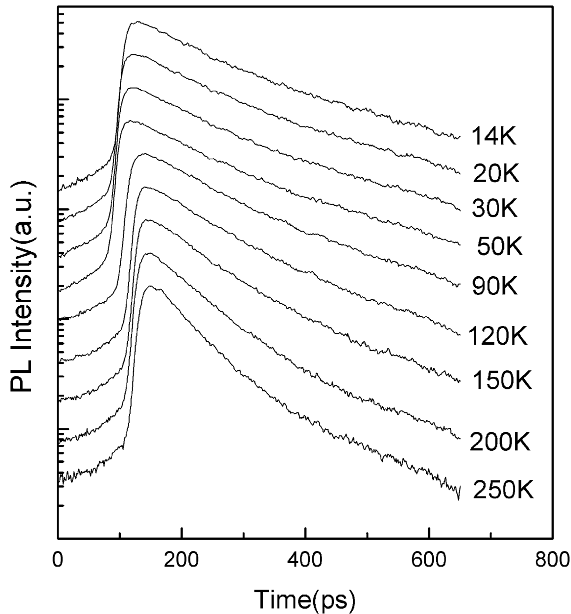

Fig. 2. Normalized PL intensity of epifilm grown directly on buffer layer at various temperatures as a function of time after excitation.

Optical properties of the InAlGaN film grown directly on buffer are further investigated with temperature-dependent PL and TRPL measurements. The PL transients from Sample No. Y0230 (Fig. 2). exhibit a strong non-exponential decay behavior at various temperatures, which implies that the emission is from certain localized states. To analyze these data, we have adopted the *stretched-exponential* law [15, 16]

$$I(t) = I_0 \exp\left[-\left(\frac{t}{\tau}\right)^{\beta}\right], \quad (1)$$

where $I(t)$ is the PL intensity as a function of time and I_0 is the intensity of $t=0$; β is a dispersive exponent and τ is the initial lifetime where the carrier density is the highest. Chen et al [17] have firstly observed the *stretched-exponential* PL decay in a low-dimensional disorder semiconductor. This decay behavior is very commonly used to describe PL decay from porous silicon or nanosilicon [15,16] and now there is growing evidence that *stretched-exponential* decay adequately models the PL decay from InGaN [18–20] under a variety of condition. Theoretical models for *stretched-exponential* behavior include either energetic or topological disorder [17, 21]. It is well known that carrier diffusion among different spatial regions can be due to the excitation of carriers from localized to extended states (energetic disorder) or to hopping of electrons among localized states (topological disorder). In the first case, the localized states play a role of *temporary traps* and the disorder results in a distribution of release rates and of trap energies; the diffusion originates from a multiple trapping–detrapping (MTD) mechanism; in the latter case, the diffusion results from hopping (H) mechanism. For the quaternary InAlGaN, which is InGaN-like alloy [22], nanoscale fluctuations in the local indium concentration are expected to form easily, which can produce both energetic and topological disorders. Therefore, the carriers recombination is probably determined by either MTD or H mechanism or even both of them. Further evidence of indium phase segregation is found by HRTEM image (Fig. 3). A random and inhomogeneous distribution of indium clusters (dark zone) is clearly observed.

To reveal which mechanism dominates the carriers recombination, we consider the dependence of β on temperature. Here β can be

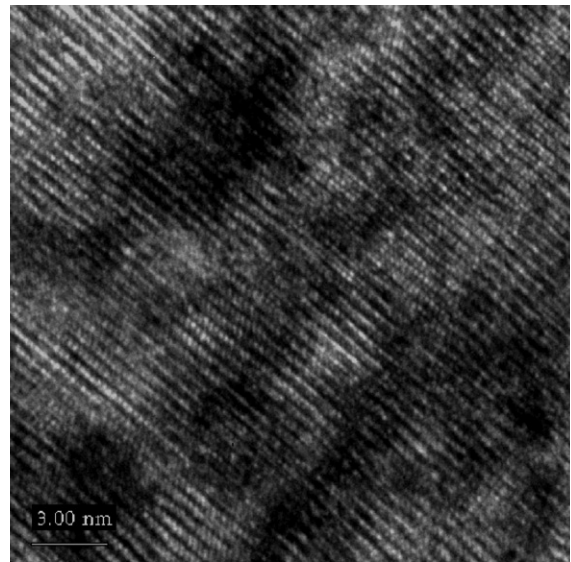

Fig. 3. A cross-sectional HRTEM image of the film.

determined by plotting $\left[dI(t)/dt\right]/I(t)$ against t in a log–log scale; from Eq. (1) the following expression could be deduced:

$$\ln\left[-\frac{dI(t)/dt}{I(t)}\right] = (\beta - 1)\ln(t) + \ln\left(\frac{\beta}{\tau^{\beta}}\right). \quad (2)$$

According to Eq. (2), β is reached from the slope of the log–log plot of $\left[dI(t)/dt\right]/I(t)$ against t. The corresponding values of the temperature-dependent β are given in Fig. 4. It demonstrates that β increases approximately linearly with temperature. Theory predicts for β a temperature independence for the H mechanism and a linear increase with temperature when the MTD mechanism dominates [23], so we can conclude that the MTD mechanism dominates the diffusion in our sample. And the In nanoclusters in the epilayer act as *temporary traps* for excitons and thus limit carriers motion.

Fig. 5 shows the temperature dependence of radiative and nonradiative recombination lifetimes (τ_r and τ_{nr}). They are deduced from the longer component of the PL decay (τ_{PL}) and the PL intensity as a function of temperature using the equation $\eta_{int} = 1/(1 + \tau_r/\tau_{nr})$, where η_{int} is an internal quantum efficiency. To simplify, η_{int} is set to unity at LT (here 14 K) since the non-radiative recombination process is generally frozen at LT. Then, τ_r and τ_{nr} can be expressed

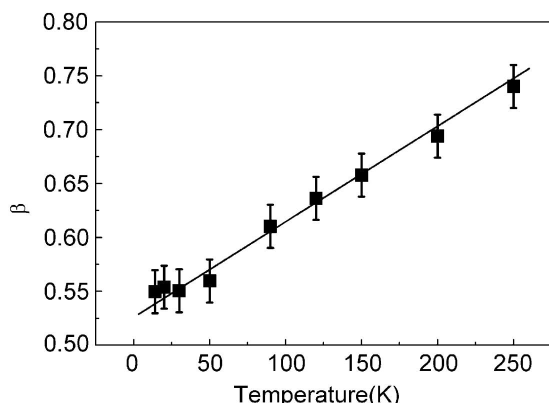

Fig. 4. The temperature-dependent β for Sample No. Y0230. The line through the β values is only a guide for the eyes.

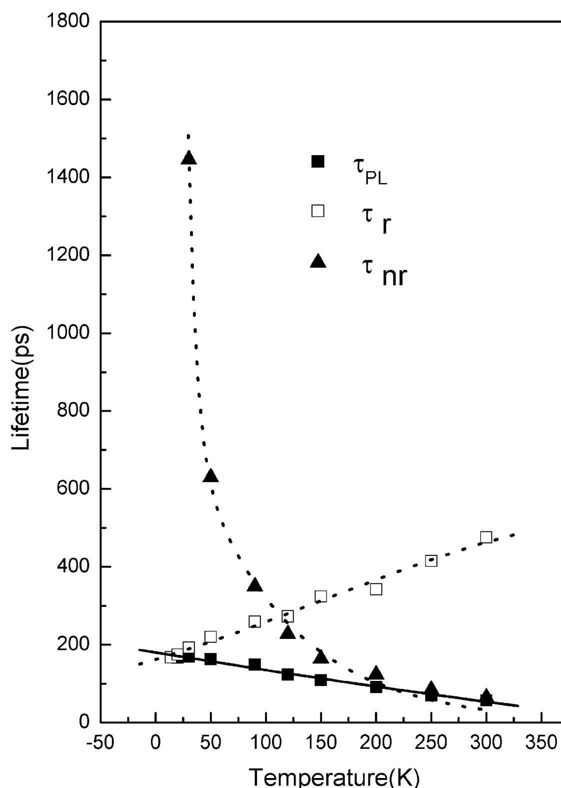

Fig. 5. PL lifetime τ_{PL} and radiative and nonradiative lifetime (τ_r and τ_{nr}) deduced from the temperature-dependent TRPL data and PL intensity.

as follows:

$$\tau_r(T) = \frac{I(14K)}{I(T)}\tau(T), \quad (3)$$

$$\tau_{nr}(T) = \frac{I(14K)}{I(14K) - I(T)}\tau(T). \quad (4)$$

Using Eqs. (3) and (4), temperature dependence of τ_r and τ_{nr} can be obtained. It can be recognized from Fig. 5 that τ_r increases linearly with temperature. Theoretically, as the confinement is smaller, i.e., the dimension is larger, the temperature-dependent radiative lifetimes increase with raising temperature. For example, for quantum dots (0D), τ_r is independent of temperature. For Q-disks (2D), however, τ_r increases linearly with temperature [24]. Therefore, the localized excitons of Sample No. Y0230 characterize 2D density of states (DOS) even at 250 K, which means

nanostructures such as Q-disks are formed in InAlGaN film. The size of the lateral In-rich region, observed by HRTEM, is smaller than 50 nm. Therefore, the size of lateral localization can be estimated to be smaller than 50 nm, and thus we can confirm the nanostructures to Q-disk size [25].

4. Conclusion

Good-quality quaternary InAlGaN film was grown directly on top of the thin LT-GaN buffer layer with (0 0 0 1)-face sapphire substrate. Temperature-dependent PL and TRPL measurements were carried out to study the carrier recombination dynamic in the quaternary film. The TPRL decay was well fitted as a *stretched-exponential* decay from 14 to 250 K. The results suggested that the emission is attributed to the radiative recombination of excitons localized in disorder quantum nanostructures such as Q-disks originating from In clusters or In composition fluctuation. The HRTEM image also demonstrates that there exist the disorder quantum nanostructures in the quaternary. By investigating the relationship of β with temperature, it is seen that the MTD mechanism dominates the diffusion among the localized states. The localized states were considered to have 2D DOS at 250 K, since τ_r increased linearly with increasing temperature.

Acknowledgements

The authors would like to thank Dr. Qingyu Xu for HRTEM measurement. This work is financially supported by the special funds for Major State Basic Research Project No. G200000683-6 and No. G001CB3095 of China and by the National Natural Science Founds of China No. 69906002. A part of the experiments was carried out at Beijing Synchrotron Radiation Facility (BSRF) of Institute of High Energy, Chinese Academy of Sciences.

References

[1] S. Nakamura, S. Pearton, G. Fasol, The Blue Laser Diode: The Complete Story, Springer, New York, 2000.
[2] I. Akasaki, H. Amano, Y. Koide, K. Hiramatsu, N. Sawaki, J. Crystal Growth 98 (1989) 209.
[3] Z. Sitar, L.L. Smith, F. Davis, J. Crystal Growth 141 (1994) 11.
[4] S.J. Pearton, J.C. Zolper, R.J. Shul, F. Ren, J. Appl. Phys. 86 (1999) 1.
[5] S. Nakamura, M. Senoh, N. Iwasa, S. Nagahama, Jpn. J. Appl. Phys. 34 (1995) L797.
[6] H.S. Kim, R.A. Mair, J. Li, J.Y. Lin, H.X. Jiang, Appl. Phys. Lett. 76 (2000) 1252.
[7] H.S. Kim, J.Y. Lin, H.X. Jiang, Appl. Phys. Lett. 73 (1998) 3426.
[8] M. Asif Khan, J.W. Yang, G. Simin, et al., Appl. Phys. Lett. 76 (2000) 1161.
[9] F.G. Mclntosh, K.S. Boutros, J.C. Roberts, et al., Appl. Phys. Lett. 68 (1996) 40.
[10] T.N. Oder, J. Li, J.Y. Lin, H.X. Jiang, Appl. Phys. Lett. 77 (2000) 791.
[11] A.P. Lima, C.R. Misky, U. Karrer, et al., J. Crystal Growth 220 (2000) 341.
[12] G. Tamulaitis, K. Kazlauskas, S. Jursenas, A. Zukauskas, Appl. Phys. Lett. 77 (2000) 2136.
[13] Mee-Yi Ryu, C.Q.Chen, E. Kuokstis, J.W. Yang, G. Simin, M. Asif Khan, Appl. Phys. Lett. 80(2002) 3730.
[14] P.D. Han, Z.G. Wang, X.F. Duan, Z. Zhang, Appl. Phys. Lett. 78 (2001) 3974.
[15] L. Pavesi, M. Ceschini, Phys. Rev. B 48 (1993) 17625.
[16] A.Yu. Kobitski, K.S. Zhuravlev, Phys. Rev. B 63 (1993) 115423.
[17] X. Chen, B. Henderson, K.P. O'Donnell, Appl. Phys. Lett 60 (1992) 2672.
[18] T.Y. Lin, J.C. Fan, Y.F. Chen, Semicond. Sci. Technol. 14 (1999) 406.
[19] M. Pophristic, F.H. Long, J. Appl. Phys. 86 (1999) 1114.
[20] S.F. Chichibu, M. Sugiyama, T. Onuma, Appl. Phys. Lett 79 (2001) 4319.
[21] H. Scher, M.F. Shlesinger, J.T. Bender, Phys. Today 26 (1991) 24.
[22] J. Li, B. Nam, K.H. Kim, J.Y. Lin, H.X. Jiang, Appl. Phys. Lett 78 (2001) 61.
[23] J. Kakalios, R.A. Street, W.B. Jackson, Phys. Rev. Lett. 59 (1987) 1037.
[24] H. Akiyama, S. Koshiba, T. Someya, et al., Phys. Rev. Lett. 72 (1994) 924.
[25] S. Chichibu, T. Sota, K. Wada, S. Nakamura, J. Vac. Sci. Technol. B 16 (1998) 2204.